Interaction of DNA with Poly(L-Lys-L-Ala-Gly) and Poly(L-Lys-L-Ala-L-Pro). Circular Dichroism and Thermal Denaturation Studies†

Arnold M. Schwartz‡ and Gerald D. Fasman*

ABSTRACT: Complexes of DNA with polypeptides composed of Lys, Ala, and Gly in both a sequential order, poly(L-lysine-L-alanine-glycine), and a statistical distribution, poly(L-lysine^{36}-L-alanine^{28}-glycine^{36}), were prepared using gradient dialysis. These polypeptide–DNA complexes were studied using ultraviolet absorption (UV) and circular dichroism (CD) to probe the conformation, binding, and melting behavior of DNA in the complex. Complexes with the sequential polypeptide showed no structural change in the DNA; however, the complexes with the random polypeptide yield CD spectra similar to Ψ DNA [Maniatis, T., Venable, Jr., J. S., and Lerman, L. S. (1974), *J. Mol. Biol. 84*, 37]. A second sequential polypeptide, poly(L-Lys-L-Ala-L-Pro)$_n$, –DNA complex was also studied. It was found to exhibit pronounced structural changes as a function of ionic strength and polypeptide–DNA ratio, more similar to the random sequence than the ordered sequence of the Lys, Ala, Gly polymer. Thus the importance of the composition and amino acid sequence in polypeptides which bind to DNA, even in such simple systems, is demonstrated. Evidence from thermal denaturation, employing simultaneous monitoring of CD and UV changes, supports a model in which specific polypeptides cause condensation of the DNA in the complex into an asymmetric tertiary structure. The relevance of these model systems to chromatin is discussed.

The importance of protein–DNA interactions in the control and regulation of the genome in cellular metabolism, replication, and development has become evident in the past several years. The DNA-dependent RNA polymerase interaction, the T4 gene-32 protein–DNA complex, and the *E. coli* lac repressor–DNA interaction are examples of such systems. Larger biological organizations such as the ribosome and chromatin depend on protein DNA or RNA interactions. (For review, see von Hippel and McGhee, 1972.) The intricate organization of proteins and DNA in chromatin is at present vaguely understood and there is intense research activity in this area. (For review, see Elgin and Weintraub, 1975.)

The conformation of chromatin and protein–DNA complexes has been probed by utilizing circular dichroism and thermal denaturation. This laboratory has investigated the interaction of individual histones with DNA and has shown the resulting CD spectra are quite different from that found for chromatin (Adler et al., 1971, 1974, 1975a,b). Thermal hyperchromicity studies on histone–DNA complexes have demonstrated differential stabilization of the DNA depending on the nature of the histone (Ansevin et al., 1971; Ansevin and Brown, 1971; Li et al., 1974a,b; Wilhelm et al., 1974a,b).

In order to evaluate and interpret protein–DNA interactions, model studies have been pursued using synthetic polypeptides complexed with DNA. Polypeptide–DNA complexes have been investigated using poly(L-Lys) (Olins et al., 1968; Li et al., 1974b; Mandel and Fasman, 1974) and random copolymers of L-Lys and Gly (Williams and Kielland, 1975), L-Lys and L-Ala (Stokrova et al., 1975; Sponar et al., 1973; Pinkston and Li, 1974), L-Lys and L-Leu (Ong et al., 1976; Ong and Fasman, 1976), and of L-Lys and L-Val (Mandel and Fasman, 1974, 1976). These latter papers from this laboratory (Mandel and Fasman, 1976; Ong and Fasman, 1976) have considered the effects of a basic polypeptide, containing a second amino acid which promotes either the β- or α-helical conformation. Sequential copolymers containing L-Lys, L-Ala, L-Pro, Gly (Sponar and Fric, 1972; Sponar et al., 1973, 1975), L-Lys, Gly (Brown et al., 1974), and L-Lys and L-Ala (Privat et al., 1972) have also been studied.

This paper reports the interaction of calf thymus DNA with both sequential and random copolymers of L-Lys, L-Ala, and Gly, and a sequential copolymer of L-Lys-L-Ala-L-Pro. These three polymers, the sequential polymer (L-Lys-L-Ala-Gly)$_n$, the statistical polymer (L-Lys^{36}-L-Ala^{28}-Gly^{36})$_n$, and the sequential polymer (L-Lys-L-Ala-L-Pro)$_n$ are models for histones (Cernosek et al., 1974a,b), in that these amino acids predominate in the histones, and especially in H1. Using the technique of Mandel and Fasman (1974), which simultaneously monitors the UV and CD thermal denaturation profile of DNA–copolymer complexes, the nature of DNA stabilization in the complex, the contribution of amino acid sequence to complex behavior, and the similarity of this model system to the melting of nucleohistone was investigated.

Materials and Methods

DNA. Calf thymus DNA, with an average molecular weight of 10×10^6, was prepared by the ethanol extraction procedure described by Adler et al. (1971). The concentration of stock solutions was determined by the ultraviolet absorbance at 258 nm, using an extinction coefficient of 6800 cm per mol per nucleotide residue (Adler et al., 1971).

Polypeptides. The synthesis and characterization of the sequential and random polypeptides of L-Lys, L-Ala, and Gly [poly(L-Lys-L-Ala-Gly), (L-A-G)$_n$; poly(L-Lys^{36}-L-Ala^{28}-

† This is Publication No. 1087 from the Graduate Department of Biochemistry, Brandeis University, Waltham, Massachusetts 02154. *Received March 8, 1976.* This research was generously supported in part by Grants from the United States Public Health Service (GM 17533), National Science Foundation (GB 29204X), and the American Cancer Society (P-577).

‡ Postdoctoral Trainee of the National Institutes of Health (Training Grant No. NS-05241-16).

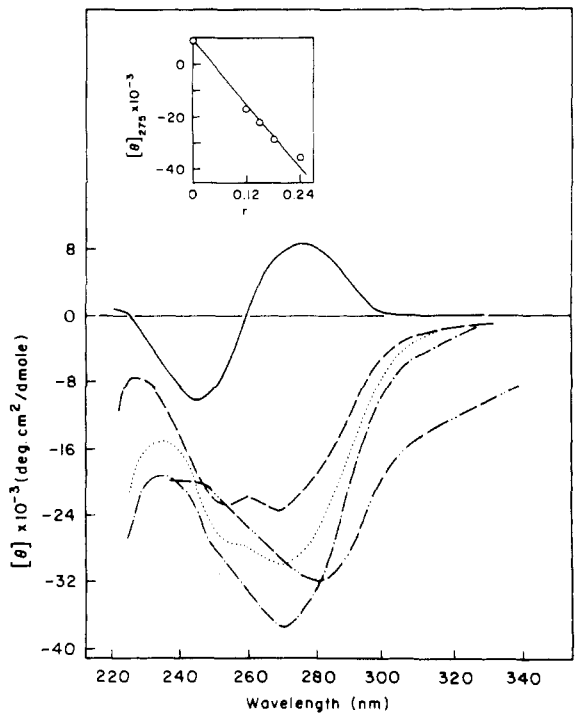

FIGURE 1: Circular dichroism spectra of (L-Lys$^{35.9}$-L-Ala$^{27.8}$-Gly$^{36.3}$)$_n$-DNA complexes at various ratios (r) in 0.14 M NaCl (pH 7.0)-10^{-3} M EDTA, 21 °C. Ratios: r = 0 (—); r = 0.145 (- - -); r = 0.175 (· · · ·); r = 0.24 (- · -); and r = 0.3 (- · · · · -). Insert: $[\theta]_{275}$ vs. r. r = Lys/nucleotide ratio.

Gly^{36}), (LAG)$_n$] and the sequential polymer, poly(L-Lys-L-Ala-L-Pro) [(L-A-P)$_n$], have been previously reported (Cernosek et al., 1974a,b). Nessler micro-Kjeldahl nitrogen analysis (Lang, 1958) was used to determine the concentration of the stock solutions of the synthetic polypeptides. Amino acid analysis on the random polypeptide showed the composition to be (Lys$^{35.9}$-Ala$^{27.8}$-Gly$^{36.3}$). The composition of the sequential polymers (L-A-G)$_n$ was 1:1:1, while that for (L-A-P)$_n$ was found to be 1.0:0.97:0.91. The weight-average molecular weight for (L-A-P)$_n$ was reported to be 27 000 (Cernosek et al., 1974b).

Polypeptide-DNA Complexes. GdmHCl[1] Dialysis. The polypeptide-DNA complexes were prepared as follows: the polypeptide and DNA were mixed in 1.5 M GdmHCl (Research Plus Laboratories, Inc.)-10 $^{-3}$M EDTA, pH 7.0, and dialyzed to the desired concentration of GdmHCl using a linear or exponential dialysis (Carroll, 1971). The DNA concentration used for all complexes was $\simeq$1.5-2.0 $\times$ 10^{-4} M in nucleotide concentration, and the amount of polypeptide was added to form complexes with a desired ratio, r, lysine/nucleotide. Dialysis was carried out at 4 °C at a flow rate of 500 or 100 mL/h for linear or exponential gradients, respectively. Spectrapor 3 (Spectrum Medical Industries, Inc.) dialysis membranes, having a molecular weight cutoff of 3500, were used. The dialysis membranes were heated in a solution of 0.01 M $NaHCO_3$ and 0.01 M EDTA to just under boiling and exhaustively rinsed with distilled water.

NaCl Dialysis. The polypeptide-DNA complexes were annealed in NaCl in an analogous manner to the GdmHCl dialysis except that the polypeptide and DNA were mixed in 1.5 M NaCl-10^{-3} M EDTA, pH 7.0. Dialysis then proceeded to the desired NaCl concentration.

Complexes for Thermal Denaturation. The complexes were prepared by the GdmHCl dialysis method, dialyzing to a 0.14 M GdmHCl concentration. The complexes were then dialyzed vs. 0.14 M NaCl-10^{-3}M EDTA, pH 7.0, to remove GdmHCl. In order to further reduce the ionic strength, an additional dialysis was performed in 2.5 $\times$ 10^{-4} M EDTA, pH 7.0.

DNA Concentration in the Complexes. The concentration of DNA in the complexes was obtained by measuring the optical density of a 0.25% sodium dodecyl sulfate solution of the polypeptide-DNA complex (Shih and Fasman, 1971).

Ionic Strength. Measurement of ionic strength was performed on a Bausch & Lomb refractometer and compared with an appropriate freshly prepared standard solution.

Thermal Denaturation. Ultraviolet and CD thermal denaturation studies were performed on polypeptide-DNA complexes in 2.5 $\times$ 10^{-4} M EDTA, pH 7.0, using the method of Mandel and Fasman (1974), whereby the absorption, ellipticity, and temperature are simultaneously monitored. Calculations were performed on a PDP-10 computer with a Calcomp plotter producing melting and derivative melting profiles of absorption and circular dichroism as described previously (Mandel and Fasman, 1974).

CD Measurements. CD measurements were performed on a Cary 60 spectropolarimeter with a Model 6001 CD attachment (Adler et al., 1971).

UV Measurements. UV measurements were performed on a Cary 14 spectrophotometer.

pH Measurements. pH measurements were performed on a Radiometer pH meter 25, with a scale expander, and equipped with a GK2032 combination electrode.

Results

Complexes of (L-Lys-L-Ala-Gly)$_n$ and DNA. The polypeptide-DNA complexes of sequential (L-A-G)$_n$ and DNA were prepared by annealing from high salt (1.5 M NaCl) to moderate ionic strength, 0.14 M, pH 7.0. At ratios (r) of Lys/nucleotide of r = 0 to r = 2, all the complex solutions were clear, and optical absorption measurements at r = 2 indicated the absence of scattering (A_{320}/A_{260} = 0.01/1.0). The CD spectra of the (L-A-G)$_n$-DNA complexes, in the range of r = 0 to r = 2, show little CD change (not shown).

At the ratio of r = 2 where there is an average of six amino acids/nucleotide, the CD spectrum is conservative in the DNA absorption band. The various spectra deviate from one another only below 230 nm due to the CD contribution from the increasing amounts of added polypeptide. The same conservative DNA CD spectra was obtained when complexes were annealed by dialysis in NaCl without GdmHCl.

Complexes of (L-Lys$^{35.9}$-L-Ala$^{27.8}$-Gly$^{36.3}$)$_n$ and DNA. When the random copolymer (LAG)$_n$ was annealed to DNA with a ratio of Lys/nucleotide in excess of 0.6, the complexes precipitate and the supernatant of such complexes, after centrifugation, show negligible optical density. Complexes of (LAG)$_n$-DNA at r = 0.3 were cloudy, and large scattering effects were apparent in the absorption spectrum, A_{350}/A_{260} = 0.35/1.5. The CD spectra of a series of complexes of (LAG)$_n$-DNA, at 0.14 M NaCl, pH 7.0, 10^{-3} M EDTA, at various ratios, are presented in Figure 1. With increasing amounts of polypeptide to DNA, the amplitude of the negative CD band at 275 nm increases and at r = 0.24, $[\theta]_{275}$ =

[1] Abbreviations used: (L-A-G)$_n$, sequential poly(L-lysine-L-alanine-glycine); (LAG)$_n$ statistical poly(L-lysine^{36}-L-alanine^{28}-glycine^{36}); (L-A-P)$_n$, poly(L-Lys-L-Ala-L-Pro); CD, circular dichroism; GdmHCl, guanidinium hydrochloride; EDTA, ethylenediaminetetraacetate; A_λ, absorbance at wavelength λ; dh_{280}/dT, thermal derivative of hyperchromicity at 280 nm; $[\theta]$, ellipticity; UV, ultraviolet.

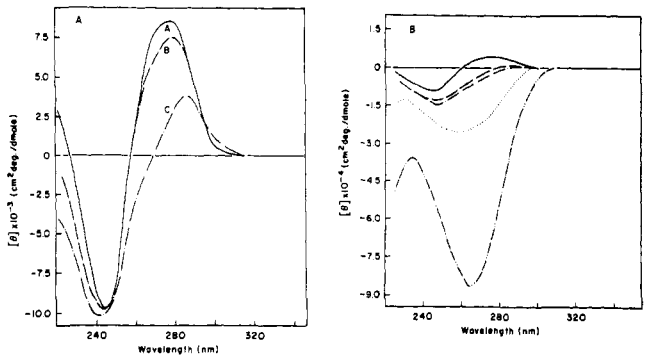

FIGURE 2: (Panel A) Circular dichroism spectra of poly(L-Lys-L-Ala-L-Pro)-DNA complexes at various ratios (r) in 0.14 M NaCl (pH 7.0)-10^{-3} M EDTA, 21 °C. The complexes were dialyzed from 1.5 M GdmHCl to 0.15 M GdmHCl by an exponential gradient and GdmHCl exchanged by NaCl. Ratios: (A (—)) $r = 0$; (B (- - -)) $r \approx 0.5$; (C (- · - · -)) $r = 1.0$. (Panel B) Circular dichroism spectra of poly(L-Lys-L-Ala-L-pro)-DNA, $r = 1$, at various GdmHCl concentrations obtained in a GdmHCl dialysis (see Materials and Methods). GdmHCl concentrations: (—) 0.17 M; (- - -) 0.15 M; (- · - · -) 0.13 M; (· · ·) 0.11 M; (- · · · · -) 0.02 M.

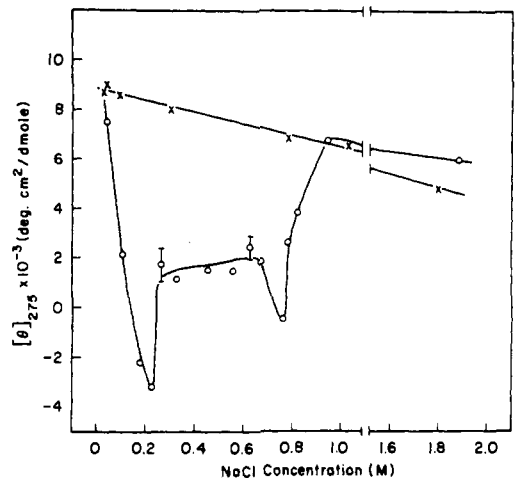

FIGURE 3: $[\theta]_{275}$ vs. NaCl concentration for complexes of (L-Lys-L-Ala-Gly)$_n$-DNA, $r = 1$, and complexes of (L-Lys$^{35.9}$, L-Ala$^{27.8}$, Gly$^{36.3}$)$_n$-DNA, $r = 0.24$. The complexes were dialyzed from 2.0 M NaCl-10^{-3} M EDTA (pH 7.0) in a linear gradient dialysis to the indicated concentrations. At various intervals, sample complexes were removed and CD spectra taken. (X—X) (L-Lys-L-Ala-Gly)-DNA; (O—O) (L-Lys$^{35.9}$, L-Ala$^{27.8}$, Gly$^{36.3}$)$_n$-DNA. r = Lys/nucleotide ratio.

$-36\,500$ deg cm^2 dmol^{-1}. The positive DNA band at 275 nm is absent at all ratios measured and is replaced with a negative band near this wavelength, which is red shifted with increasing polypeptide to DNA ratios, and a band near 245 nm appears. Similarly, the magnitude of the CD band at 245 nm increases with r and also shifts toward the red; this CD band becomes dominated by the negative 270-nm CD band at $r = 0.24$. At $r = 0.3$, the $[\theta]_{280}$ band ($-32\,000$ deg cm^2 dmol^{-1}) of the (LAG)$_n$-DNA complex is reduced in magnitude compared with $r = 0.24$ and is red shifted. This solution of the (LAG)$_n$-DNA complex was quite turbid and displayed optical scattering as evidenced by $A_{350}/A_{260} = 0.55/1.22$.

Complexes of Poly(L-Lys-L-Ala-L-Pro)-DNA. The CD spectra of polypeptide-DNA complexes, in 0.14 M NaCl-10^{-3} M EDTA, pH 7.0, are presented in Figure 2A. As the lysine/nucleotide ratio, r, is increased, the positive CD band at 275 nm decreases in magnitude and both the crossover point and ellipticity maximum are red-shifted. The maximum ellipticity at $r = 0.5$ is 7500 deg cm^2 dmol^{-1} at 280 nm and at $r = 1.0$ is 3880 deg cm^2 dmol^{-1} at 285 nm. These solutions show scattering in their absorption spectra, $A_{350}/A_{260} = 0.26/1.18$ for $r = 1.0$. At ratios of lysine/nucleotide above 1.2, the complex precipitated and the supernatant of such complexes after centrifugation showed little DNA present.

The CD spectra of the (L-A-P)$_n$-DNA complex, $r = 1$, at concentrations of GdmHCl of 0.23 M and below are presented in Figure 2B. At the higher salt concentrations ($\geq$0.3 M), the CD spectra of the polypeptide-DNA complex yield a similar pattern to that observed with DNA alone (not shown); as the GdmHCl concentration is lowered, the positive CD band at ~275 nm increases in magnitude and the crossover point shifts toward the blue (not shown). As the GdmHCl concentration decreases below 0.2 M, the positive CD band vanishes and the spectrum is dominated by a large negative band at 245 nm; $[\theta]_{245} = -14\,000$ deg cm^2 dmol^{-1} in 0.13 M GdmHCl. This negative CD band further decreases and red-shifts as the concentration of salt is further lowered; $[\theta]_{260} = -25\,000$ deg cm^2 dmol^{-1}, 0.11 M GdmHCl, and $[\theta]_{265} = -86\,700$ deg cm^2 dmol^{-1}, 0.02 M GdmHCl.

Effect of Ionic Strength on the Polypeptide-DNA Complexes. (L-A-G)$_n$. The effect of varying the salt concentration on the polypeptide-DNA complexes was investigated by monitoring the CD of the complex at various salt concentrations during a linear salt gradient dialysis. These experiments were performed using either GdmHCl or NaCl. The curve for the complex of sequential (L-A-G)$_n$ polypeptide with DNA, at $r = 1$, linearly increases with decreasing salt to the B-form CD spectra of DNA (Figure 3, $[\theta]_{275}$ vs. the NaCl concentration). The major CD spectral change of the complex with varying NaCl concentration occurs in the positive CD band at 275 nm. There is also a change in the crossover point from 260 nm, at high salt (1.79 M), to 257 nm, at low salt (0.04 M). The absorption spectra and the CD negative band at 245 nm showed no salt dependence.

(LAG)$_n$. When the CD curve of the random (LAG)$_n$-DNA complex is monitored at different NaCl concentrations, pronounced CD spectral changes occurred. At $r = 0.24$, $[\theta]_{275}$ initially increases with decreasing salt, similar to the (L-A-G)$_n$-DNA complex, but then decreases sharply at 0.9 M NaCl. The positive CD band of the DNA is red shifted as the salt concentration is lowered and the magnitude decreases until it is nearly zero at 0.18 M. The crossover point also shifts from 259 nm, at 0.96 M, to 288 nm, at 0.18 M NaCl. With decreasing NaCl concentrations, the negative CD band (~245 nm) shifts toward the red and increases in magnitude. At 0.18 M NaCl, a slight shoulder is observed at 270 nm. As the salt gradient continues below 0.18 M NaCl, the CD spectral characteristics return to that of B-form DNA. The positive CD band increases with decreasing salt (below 0.16 M NaCl) and is blue shifted, and the crossover point returns to 257 nm at 0.012 M NaCl. A graph of $[\theta]_{275}$ as a function of the NaCl concentration for the (LAG)$_n$-DNA complex is seen in Figure 3. Unlike the linear relation observed for the sequential (L-A-G)$_n$-DNA complex, the plot of $[\theta]_{275}$ vs. [NaCl] has two minima for the random (LAG)$_n$-DNA complex. At the extremes of the salt concentration studied, the $[\theta]$ values are approximately equal for both systems. This suggests that, in the two polypeptide systems, at high salt where no binding occurs, and at low salt where binding occurs, the DNA has a similar structure. In the intermediate range of salt concentration, two minima occur approximately at 0.75 and at 0.22 M NaCl. These experiments were repeated using an expo-

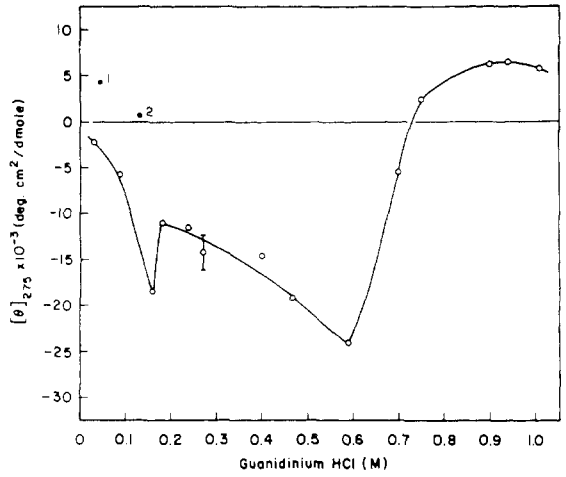

FIGURE 4: $[\theta]_{275}$ vs. GdmHCl concentration for the (L-Lys$^{35.9}$, L-Ala$^{27.8}$, Gly$^{36.3}$)$_n$-DNA complex, at r = 1. Procedures as in Figure 3, except GdmHCl was used rather than NaCl. Points 1 and 2 represent a step dialysis from 1.01 and 0.75 M GdmHCl, respectively.

nential gradient to rule out any artifacts which the dialysis may have produced (i.e., the double minima salt dependence), and similar results were obtained.

The effect of varying the salt concentration on the CD spectra of the (LAG)$_n$-DNA complex at r = 0.24 was also determined, using a gradient dialysis with GdmHCl. The same experimental conditions were followed as above, except that NaCl was replaced by GdmHCl. A series of CD spectra of the complex, at different concentrations of GdmHCl, was obtained (not shown). As the concentration of GdmHCl decreases, the positive CD band decreases and red shifts, similar to the CD spectral curves of the complex in NaCl. However, in the presence of GdmHCl, the CD spectral changes are more pronounced. Most significant is the appearance of the dominant negative CD band at $\simeq$270 nm which increases as the concentration of GdmHCl is lowered until 0.59 M (Figure 4). In addition, the negative band at 245 nm shifts toward the red with decreasing GdmHCl. As the GdmHCl concentration is further lowered (between 0.59 and 0.17 M), the negative band at 275 nm decreases in magnitude to a value of $[\theta]_{275}$ = $-11\,000$ at 0.17 M. On lowering the GdmHCl concentration to 0.16 M, an extremum is found with $[\theta]_{275} = -18\,800$ deg cm^2 dmol^{-1}. On further decreasing the GdmHCl concentration below 0.16 M, the CD spectrum of the (LAG)$_n$-DNA complex does not return to the B-form DNA CD spectrum, even at GdmHCl concentrations in the mM range. In the case of the (LAG)$_n$-DNA complex dialyzed in NaCl, however, the CD spectrum at low salt was identical with that of DNA alone in dilute ionic strength media. The change in $[\theta]_{275}$ at varying GdmHCl concentrations is seen in Figure 4. As in the case of the dialysis of the complex in NaCl (Figure 3), two minima are present; however, the respective minima occur at a lower concentration in the GdmHCl dialysis than in the NaCl dialysis. Moreover, the high ionic strength extremum in the GdmHCl dialysis is quite broad and the ellipticity values are significantly more negative than those in the NaCl dialysis: $[\theta]_{275} = -24\,600$ deg cm^2 dmol^{-1} in 0.59 M GdmHCl, whereas $[\theta]_{275} = -1500$ deg cm^2 dmol^{-1} in 0.75 M NaCl. In contrast, the extremum at low GdmHCl concentration (0.16 M) is sharper than the respective extremum for the NaCl dialysis (0.22 M NaCl) and, contrary to the NaCl dialysis, the low ionic strength minimum has a smaller negative ellipticity value than the higher ionic strength minimum.

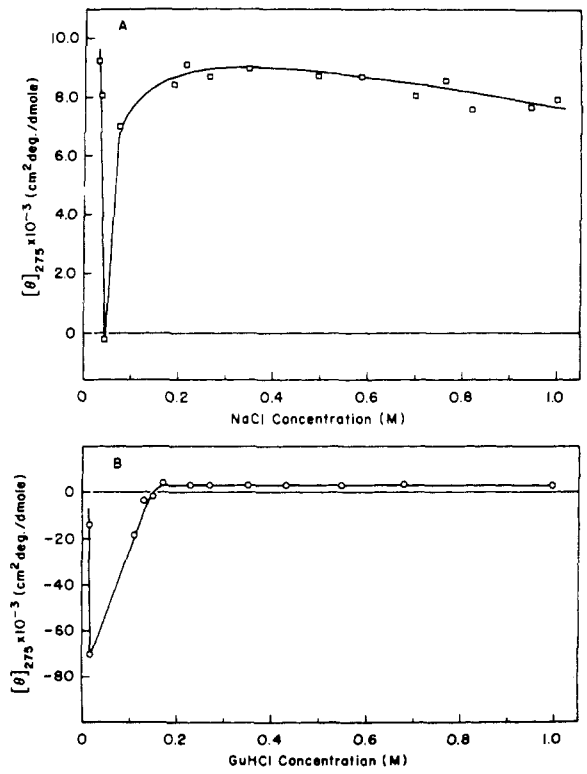

FIGURE 5: (A) $[\theta]_{275}$ vs. NaCl concentration for complexes of poly(L-Lys-L-Ala-L-Pro)-DNA, r = 1. The complexes were dialyzed from 1.5 M NaCl-10^{-3} M EDTA (pH 7.0) in a linear gradient dialysis to the indicated concentrations. At these points, sample complexes were removed and CD spectra taken. (B) $[\theta]_{275}$ vs. GdmHCl concentration for complexes of poly(L-Lys-L-Ala-L-Pro)-DNA, r = 1. Procedure as in A.

The complexes studied in the gradient dialysis experiments were exposed to a continuous decrease in salt concentration. If the salt environment was changed abruptly, as in a step dialysis, different CD spectral changes with varying salt occurred. As seen in Figure 4, the points 1 and 2 are respectively the ellipticity values, $[\theta]_{275}$, for complexes obtained from step dialysis at 1.01 and 0.75 M GdmHCl.

(L-A-P)$_n$. In order to investigate the effect of ionic strength on a (L-A-P)$_n$-DNA complex, r = 1, the CD spectra of the complex was monitored at various salt concentrations during a gradient dialysis. These experiments were performed with either NaCl or GdmHCl. A plot of $[\theta]_{275}$ vs. NaCl concentration is shown in Figure 5A. A linear increase of the ellipticity of the complex vs. decreasing salt is found from 1.0 to $\sim$0.2 M NaCl. As the complex is dialyzed to still lower salt concentrations (<0.2 M NaCl), the ellipticity sharply decreases to a value of $[\theta]_{275} \simeq -1200$ deg cm^2 dmol^{-1} at $\sim$0.04 M NaCl and then rises and returns to the usual B-form CD spectrum of DNA at salt concentrations below 0.01 M NaCl.

The dependence of the CD spectra of the (L-A-P)$_n$-DNA complex, r = 1, on ionic strength was also studied using GdmHCl in the gradient dialysis. As seen in Figure 5B, $[\theta]_{275}$ vs. the GdmHCl concentration, a similar result to the NaCl dialysis is obtained. As the GdmHCl concentration is reduced from 1.0 to $\sim$0.2 M, the ellipticity increases linearly, analogous to the salt effect on DNA alone. Below 0.2 M GdmHCl, the ellipticity decreases and reaches a maximum negative value at 0.02 M GdmHCl, where $[\theta]_{275} = -71\,000$ deg cm^2 dmol^{-1}. Below this ionic strength, the value of the ellipticity at 275 nm rises; $[\theta]_{275} = -14\,000$ deg cm^2 dmol^{-1} at 0.015 M GdmHCl. At lower salt concentrations, the CD spectrum of the complex

TABLE I: Melting Temperatures for Polypeptide-DNA Complexes at Various Ratios (r).[a]

Complex	r[a]	T_{mI}[c] UV	T_{mI}[c] CD	T_{mII}[c] UV	T_{mII}[c] CD	$T_{mII'}$[c] UV	$T_{mII'}$[c] CD	T_{mIII}[c] UV	T_{mIII}[c] CD
I (poly(L-Lys-L-Ala-Gly)-DNA)	0	48	49						
	0.5	52.5	52	66	62			77	74
	1	53	54	66	66			77	72
	1.5	57		67.5	69.5			77	76
	2							76[b]	78[b]
II (poly(L-Lys$^{35.9}$-L-Ala$^{27.8}$Gly$^{36.3}$)-DNA)	0	48	49						
	0.145	54	54	61	68	76	85	92	94
	0.175	53	53	62	62	75	85	92	93
	0.24	58	58	70	68	76	86	91	93

[a] r = ratio = lysine/nucleotide. [b] High melting tail region. [c] In °C.

does not return to the B-form DNA spectra. In the GdmHCl dialysis, the transition occurs over a wider salt concentration, the ellipticity at the minimum is almost two orders of magnitude greater than found in the NaCl dialysis, and the minimum of the CD dependence on ionic strength occurs at a lower GdmHCl concentration (0.02 M) than NaCl concentration (0.04 M).

The effect of ionic strength on the $(L\text{-}A\text{-}P)_n$-DNA complexes described above has been studied using a gradient dialysis system of GdmHCl or NaCl. If the particular salt is changed in the region where binding occurs, while the overall salt concentration is maintained, marked CD changes are noted. Thus, when the $(L\text{-}A\text{-}P)_n$-DNA complex is dialyzed down from 1.5 M GdmHCl to 0.15 M GdmHCl and the GdmHCl is replaced with 0.15 M NaCl, the $[\theta]_{275}$ changes from -8000 deg cm^2 dmol^{-1} (0.15 M GdmHCl) to $+1200$ deg cm^2 dmol^{-1} (0.15 M NaCl). When the dialysis from GdmHCl to NaCl is performed at the minimum observed in Figure 5B, at 0.02 M GdmHCl, the change is more pronounced; $[\theta]_{275} = -71\,000$ deg cm^2 dmol^{-1} in GdmHCl, and $[\theta]_{275} = 5500$ deg cm^2 dmol^{-1} in NaCl. This ellipticity value in NaCl is less than the value obtained when the gradient dialysis is performed in NaCl alone ($[\theta]_{275} \simeq 8000$ deg cm^2 dmol^{-1} at 0.02 M NaCl).

Thermal Denaturation. $(L\text{-}Lys\text{-}L\text{-}Ala\text{-}Gly)_n$-DNA Complexes. Complexes of $(L\text{-}A\text{-}G)_n$-DNA at various ratios (r) (0 to 2), in 2.5×10^{-4} M EDTA, pH 7.0, were thermally denatured according to the method of Mandel and Fasman (1974) (see Table I) in which the UV absorbance and CD are simultaneously measured. The derivative absorption melting profiles, dh_{280}/dT vs. temperature, are shown in Figure 6. The melting of unbound DNA occurs at 47 °C with a shoulder at 55 °C. Three melting regions are present for the sequential polypeptide $(L\text{-}A\text{-}G)_n$-DNA complexes: 45–55 °C (T_{mI}); 62–70 °C (T_{mII}); and 72–80 °C (T_{mIII}). The first melting region of the $(L\text{-}A\text{-}G)_n$-DNA complexes represents denaturation of the free DNA, in agreement with previously published results of this laboratory (Mandel and Fasman, 1974; Ong and Fasman, 1976) and consistent with the melting of DNA alone under these conditions. As the ratio of polypeptide to DNA is increased, the central melting region with $T_{mII} = 66$ °C increases in area relative to the other melting regions as seen in the differential hyperchromicity profile of Figure 6. Above $r = 1$, the highest melting region with $T_m = 77$ °C increases in area relative to the other two regions, and the central melting region then decreases. In addition, as more polypeptide is bound, the two melting regions corresponding to the free DNA region and the central region, T_{mII}, show an

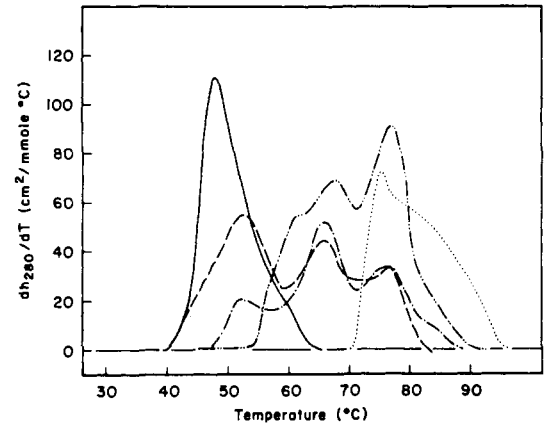

FIGURE 6: Derivative thermal hyperchromicity melting profiles, dh_{280}/dT vs. temperature of $(L\text{-}Lys\text{-}L\text{-}Ala\text{-}Gly)_n$-DNA complexes at various ratios (r). Thermal denaturation in 2.5×10^{-4} M EDTA, pH 7.0, monitored at 280 nm. Curves are first derivative of 280-nm hyperchromicity with respect to temperature. Ratios: $r = 0$ (—); $r = 0.5$ (- - -); $r = 1$ (- · - ·); $r = 1.5$ (- · · - · ·); $r = 2$ (· · · ·). r = Lys/nucleotide ratio.

increase in their respective melting temperature. The T_{mI} of free DNA region increases from 66 to 68 °C. Simultaneously, the high melting region, T_{mIII}, shows an increase in the high temperature tail of that melting zone.

The differential thermal ellipticity, $d[\theta]_{280}/dT$, melting profiles for various ratios of $(L\text{-}A\text{-}G)_n$ to DNA are shown in Figure 7. Although three melting zones are evident in the CD profiles, the respective T_m for each zone is not precisely at the same T_m obtained in the ultraviolet hyperchromism meltout, but rather, shows a dependence on the polypeptide/DNA ratio (Table I). The central melting region has a $T_{mII} = 66$ °C, for $r = 0.5$ and 1, and $T_{mII} = 68$ °C for $r = 1.5$ as monitored by dh_{280}/dT (Figure 6) and the T_{mII}'s are equal to 62, 64, and 69 °C for $r = 0.5$, 1, and 1.5, respectively, when measured in the CD mode (Figure 7). Nevertheless, the thermal derivative CD melting profiles generally agree with the results obtained by ultraviolet hyperchromism, namely, that with increasing r an intermediate melting region is initially stabilized with a $T_m \simeq 66$ °C, which decreases in relative area at higher ratios and simultaneously a high melting region with a $T_m \simeq 76$ °C develops.

Thermal Denaturation of $(L\text{-}Lys^{35.9}\text{-}L\text{-}Ala^{27.8}\text{-}Gly^{36.3})_n$*-DNA Complexes.* Complexes of $(LAG)_n$-DNA, at above $r = 0.3$, precipitate and cannot be used for optical measurements. At ratios of $r = 0.24$ and below the differential thermal melting profile in the absorption mode is quite complex (Figure

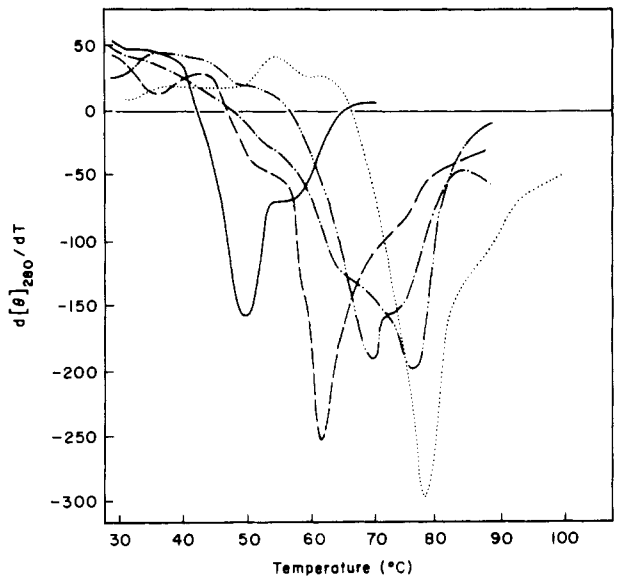

FIGURE 7: Derivative thermal circular dichroism melting profile, $d[\theta]_{280}/dT$ vs. temperature, of (L-Lys-L-Ala-Gly)$_n$-DNA complexes at various ratios. Ratios: $r = 0$ (—); $r = 0.5$ (- - -); $r = 1$ (- · - ·); $r = 1.5$ (- · · - · ·); $r = 2$ (· · · ·). r = Lys/nucleotide ratio.

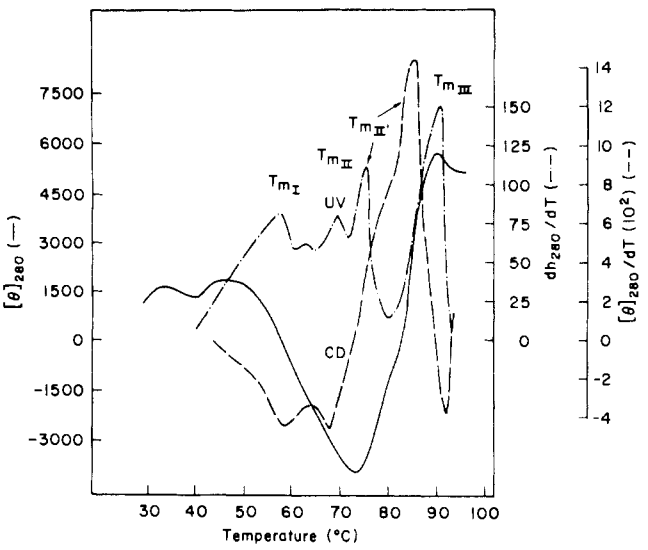

FIGURE 9: Thermal melting profiles of (L-Lys$^{35.9}$, L-Ala$^{27.8}$, Gly$^{36.3}$)$_n$-DNA complex, $r = 0.24$. Thermal denaturation in 2.5×10^{-4} M EDTA, pH 7.0. Solid line (—) represents the CD curve monitored at 280 nm vs. temperature. The derivative of the thermal hyperchromicity (dh_{280}/dT) vs. temperature (- · -) and the derivative of the thermal ellipticity ($d[\theta]_{280}/dT$) vs. temperature (- - -) are also shown.

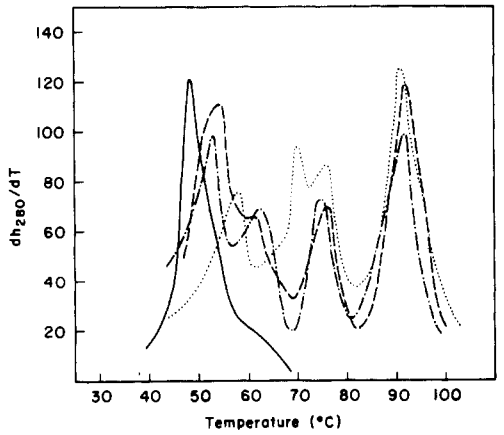

FIGURE 8: Derivative thermal hyperchromicity melting profile, dh_{280}/dT vs. temperature, of (L-Lys$^{35.9}$, L-Ala$^{27.8}$, Gly$^{36.3}$)$_n$-DNA complexes at various ratios (r). Thermal denaturation in 2.5×10^{-4} M EDTA, pH 7.0, monitored at 280 nm. Ratios: $r = 0$ (—); $r = 0.145$ (- - -); $r = 0.175$ (- · - ·); $r = 0.24$ (· · · ·). r = Lys/nucleotide ratio.

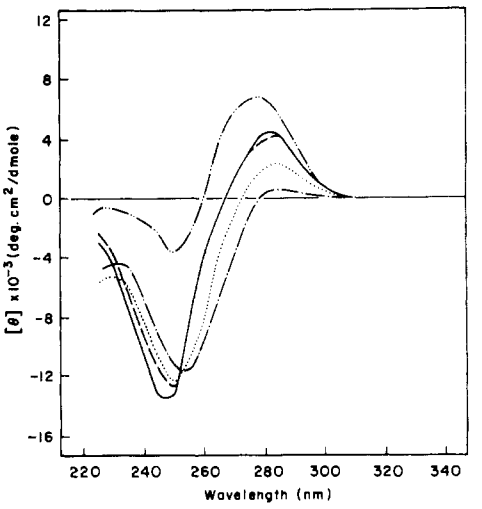

FIGURE 10: Circular dichroism spectra of the (L-Lys$^{35.9}$, L-Ala$^{27.8}$, Gly$^{36.3}$)$_n$-DNA complex at $r = 0.145$ at various temperatures. Thermal denaturation in 2.5×10^{-4} M EDTA, pH 7.0, was monitored and the CD spectra were taken at the indicated temperatures: 25 °C (—); 44 °C (- - -); 58 °C (· · · ·); 75 °C (- · -); 97 °C (- · · -).

8). At ratios as low as $r = 0.145$, the absorption melting profile shows at least four melting regions with melting temperatures of 54, 61, 76, and 92 °C (see Table I). It is probable that the random (LAG)$_n$ polypeptide binds selectively to the AT rich regions of DNA leaving the GC rich regions relatively unbound.

In order to probe structural changes in the DNA accompanying the thermal denaturation, simultaneously monitoring of the CD and UV spectra during melting has been carried out. A composite melting profile of the CD changes during melting superimposed on the thermal derivative of both UV and CD is shown in Figure 9 for the (LAG)$_n$-DNA complex at $r = 0.24$. The CD melting profile for the random polypeptide-DNA complex displays a decreasing ellipticity at temperatures above the premelting region, reaching a minimum at about 75 °C and then an increasing ellipticity with a maximum at 90 °C.

To gain added insight into the process of the thermal denaturation of the complex, the CD spectra of the (LAG)$_n$-DNA complex, $r = 0.145$, has been measured at various temperatures (Figure 10). As the temperature is raised, the major CD change occurs in the positive 280-nm CD band. From 25 to 75 °C, this band continuously diminishes and both the positive CD band and crossover point are red-shifted, while the negative 245-nm band is slightly red shifted and decreases slightly in magnitude. The resulting CD spectrum at 75 °C has the appearance of a room-temperature spectra of the complex at moderate salt concentrations (Figure 5B). This CD spectrum probably indicates the residual ordered structure of the DNA in the complex present at 75 °C. With an increase in temperature, this structure is also melted and, by 97 °C, the entire complex is denatured, probably into single DNA strands. The thermal denaturation profiles of (LAG)$_n$-DNA complexes not only reveal the melting of free DNA and polypeptide bound DNA secondary structure, but demonstrate the exis-

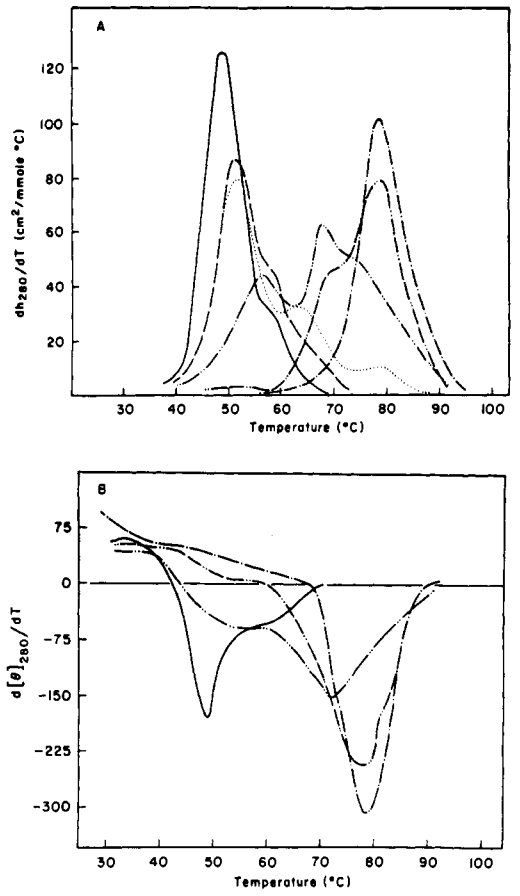

FIGURE 11: (A) Derivative thermal hyperchromicity melting profiles, dh_{280}/dT vs. temperature, of poly(L-Lys-L-Ala-L-Pro)-DNA complexes at various ratios (r). Thermal denaturation in 2.5×10^{-4} M EDTA, pH 7.0, is monitored at 280 nm. Ratios: (—) $r = 0$; (- - -) $r = 0.07$; (· · · ·) $r = 0.18$; (- · · · · ·) $r = 0.4$; (- · · · · · · ·) $r = 0.8$; (- · -) $r = 1.2$. (B) Derivative thermal circular dichroism melting profile, $d[\theta]_{280}/dT$ vs. temperature, of poly(L-Lys-L-Ala-L-Pro)-DNA complexes at various ratios (r). Same conditions as in A. Ratios: (—) $r = 0$; (- · · · · ·) $r = 0.4$; (- · · · · · · ·) $r = 0.8$; (- · · ·) $r = 1.2$.

tence of tertiary structure in polypeptide bound-DNA regions.

Thermal Denaturation of Poly(L-Lys-L-Ala-L-Pro)-DNA Complexes. The thermal denaturation of the $(L\text{-}A\text{-}P)_n$-DNA complexes in 2.5×10^{-4} M EDTA, pH 7.0, was examined using the method of Mandel and Fasman (1974). The UV thermal derivative profiles, dh_{280}/dT vs. T, of a series of complexes at different r values (Lys/nucleotide) are shown in Figure 11A. The solutions of the polypeptide-DNA complexes were clear and showed no optical scattering; their CD spectra were all similar to the conservative B-form CD spectra of DNA alone (not shown). The melting of DNA, dh_{280}/dT, in the absence of polypeptide ($r = 0$) occurs at 47 °C with a minor shoulder at 55 °C corresponding to a region in the DNA having a higher GC content relative to the overall GC content of calf thymus DNA (Li et al., 1974). As the polypeptide, $(L\text{-}A\text{-}P)_n$, to DNA ratio is increased, the presence of three melting regions is observed: 45–55 °C (T_{mI}), 64–70 °C (T_{mII}), and 76–80 °C (T_{mIII}) (Table II). The first melting region of $(L\text{-}A\text{-}P)_n$-DNA complexes at low ratios represents the denaturation of unbound DNA in the complex and is consistent with the melting of DNA alone under these solution conditions.

As the ratio of polypeptide to DNA is increased, the presence of a central melting zone appears. This melting region

TABLE II: Melting Temperatures for Poly(L-Lys-L-Ala-L-Pro)-DNA Complexes at Various Ratios (r).

	T_{mI}[a]		T_{mII}[a]		T_{mIII}[a]	
r	UV	CD	UV	CD	UV	CD
0	48	49				
0.18	52	54	64	64	78	76
0.40	57	54	68		77	73
0.80			69		79	78
1.20					79	78

[a] In °C.

increases in fractional area with increasing r, and its melting temperature (T_{mII}) also increases with increasing Lys/nucleotide ratio. At a ratio of Lys/nucleotide = 0.4, three melting regions are observed. Above this ratio, $r = 0.8$, there is no free DNA melting region, implying that the entire DNA has been thermally stabilized by bound polypeptide. Thus a solution of $(L\text{-}A\text{-}P)_n$-DNA complex, $r = 0.8$, can be heated to 60 °C (beyond the free DNA melting region) and cooled to room temperature without any change in hypochromicity. At a ratio of 1.2, the polypeptide-DNA complex melts in a single transition (T_{mIII}) without any contribution from the central melting region.

The derivative CD melting profiles, $d[\theta]/dT$ vs. T, are presented in Figure 11B. The free DNA melting region in CD is characterized by a $T_{mI} = 47$ °C in agreement with the UV melting profile. At a ratio of Lys/nucleotide, $r = 0.18$, the derivative CD melting profile has the same three melting regions observed in the derivative UV melting profile, with melting temperatures 52 °C (T_{mI}), 65 °C (T_{mII}), and 82 °C (T_{mIII}) (not shown). At a ratio of 0.4 the derivative CD melting profile is dominated by high melting regions and a smaller free DNA melt; and at $r \geq 0.8$ there is a minimal contribution due to free DNA melting and the thermal profile is effectively characterized by the high melting zone. Thus, the general pattern of the polypeptide-DNA denaturation observed by hyperchromicity changes is consistent with the circular dichroism melt. The CD changes for all the complexes, beyond the premelting region, are monotonically decreasing in the direction of decreased asymmetry. The change in the CD magnitude from its maximum before melting to its minimum after the melt is approximately equal for all complex ratios but is larger than found for DNA alone. In addition, at all ratios a premelt is observed which generally increases with increases in Lys/nucleotide ratio.

Discussion

Circular Dichroism Spectra of Complexes. The CD spectra of complexes of DNA with sequential $(L\text{-}A\text{-}G)_n$, random $(LAG)_n$, and sequential $(L\text{-}A\text{-}P)_n$, which have been annealed by a gradient dialysis, have been presented. The CD spectra of the sequential $(L\text{-}A\text{-}G)_n$-DNA complexes do not vary with the ratio of bound polypeptide to DNA. The solutions of the $(L\text{-}A\text{-}G)_n$-DNA complex display no UV scattering, even at $r = 2$, and the CD spectra are approximately the same as that of DNA alone (above the peptide spectral region). These results indicate that the DNA interaction with sequential $(L\text{-}A\text{-}G)_n$ form complexes with little or no structural change in DNA secondary conformation, and, moreover, there is no DNA condensation, aggregation, or tertiary structural changes in the complex at all r values studied.

The random $(LAG)_n$-DNA complexes are distinctly different from the sequential $(L\text{-}A\text{-}G)_n$-DNA complexes. The $(LAG)_n$-DNA complexes at $r > 0.3$ precipitate in contrast to the soluble complexes of $(L\text{-}A\text{-}G)_n$-DNA. It is evident that it is the sequence and not the percentage of the constituent amino acids which is crucial in determining the structure of the polypeptide-DNA complex.

The CD spectra of the random $(LAG)_n$-DNA complex, at various r values, are shown in Figure 1. These CD spectra are similar to those spectra observed for other systems: complexes of DNA and block $(Lys^x)_n(Leu^y)_m$ copolymers (Ong and Fasman, 1976), complexes of DNA and sequential $(L\text{-}Ala\text{-}L\text{-}Lys\text{-}L\text{-}Pro)_n$ (Sponar et al., 1973, 1975), complexes between DNA and histone H1 (Fasman et al., 1970), complexes of poly(L-lysine) and DNA (Williams and Kielland, 1975; Mandel and Fasman, 1976), and DNA in the presence of NaCl plus either polyethylene oxide or polyacrylate (Jordan et al., 1972). In addition, these Ψ DNA like spectra (Jordan et al., 1972) are also observed with complexes of DNA and copolymers of L-lysine and L-alanine (Stokrova et al., 1975) and with copolymers of L-lysine and glycine (Williams and Kielland, 1975). From the proposed structure of Ψ DNA, and the similarity of the CD spectra presented here, it is suggested that the interaction of the random $(LAG)_n$ copolymer with DNA, in the presence of salt, causes the condensation of DNA in the complex to an ordered and asymmetric structure. This condensation is achieved by the aggregation of regions of polypeptide bound DNA on the same or different DNA molecules. The differences in the CD spectra for these various polypeptide-DNA complexes may indicate differences in the mode of polypeptide binding and degree of DNA condensation.

The plot of the $[\theta]_{275}$ vs. r (insert in Figure 1) yields a straight line which is consistent with the idea that DNA exists in two states (Pinkston and Li, 1974): one in which polypeptide bound segments induce a Ψ-like structure and the other with the remaining unbound DNA in the normal B form.

The CD spectra of the sequential $(L\text{-}A\text{-}P)_n$-DNA complexes as a function of salt and Lys/nucleotide ratio have been presented (Figures 2A and B). As the ratio of Lys/nucleotide increases at a fixed NaCl concentration (0.15 M), the positive CD band at 275 nm decreases; yet the negative CD band at 245 nm remains relatively unchanged (Figure 2A). The CD spectra of the complex at $r = 1$, in 0.04 M NaCl, manifests Ψ-like CD spectra (Jordan et al., 1972). As the concentration of the salt is decreased below this critical salt concentration, the Ψ-like CD spectral magnitudes decrease, and, in the case of varying NaCl concentration, the CD spectra return to a B-form DNA CD spectrum at low ionic strength.

The complexes formed with DNA and the sequential $(L\text{-}A\text{-}P)_n$ are quite different from those formed with sequential $(L\text{-}A\text{-}G)_n$. Though both sequential polypeptides are in the random conformation when free in solution at low and high ionic strength (Cernosek et al., 1974a,b), when bound to DNA they promote quite different structural forms of DNA. $(L\text{-}A\text{-}G)_n$-DNA complexes have CD spectra generally identical with those of DNA alone, whereas CD spectra of $(L\text{-}A\text{-}P)_n$-DNA complexes manifest Ψ-form CD spectra dependent upon salt and polypeptide concentrations. Moreover, the $(L\text{-}A\text{-}P)_n$-DNA complexes precipitate at $r > 1.2$; whereas the $(L\text{-}A\text{-}G)_n$-DNA complexes are soluble and optically clear at $r = 2$.

The compact structural form stabilized by $(L\text{-}A\text{-}P)_n$ is presumably due to interactions between bound polypeptide units on the DNA, which promote its condensation. The $(L\text{-}A\text{-}P)_n$ polypeptide has a greater potential for interpolypeptide interactions than does $(L\text{-}A\text{-}G)_n$, possibly due to the greater hydrophobicity of Pro than Gly and/or to the different geometries of the bound polypeptides. Despite the fact that both Gly and Pro have a low potential for structure formation in proteins (Chou and Fasman, 1974), Gly has considerably more conformational freedom than Pro which presumably produces different topologies of the DNA bound polypeptides.

At the extremes of NaCl concentration, the CD spectra of $(L\text{-}A\text{-}P)_n$-DNA, $r = 1$, are equal to the respective CD spectra observed for $(Lys\text{-}Ala\text{-}Gly)_n$-DNA, $r = 1$, and $(L\text{-}Lys^{35.9}\text{-}L\text{-}Ala^{27.8}\text{-}Gly^{36.3})$-DNA, $r = 0.24$. Thus, under these conditions, the $(L\text{-}A\text{-}P)_n$-DNA complex presumably has a similar DNA structure to the polypeptide-DNA systems studied previously at high salt where no binding occurs, and at low salt even though binding is complete.

The sequential and statistical polypeptides of Lys, Ala, Gly differ in their interactions with DNA. These differences are probably a result of the different amino acid distributions in these polypeptides and, therefore, different conformations when bound to DNA. It is clear that the sequential copolymer has a unique amino acid sequence with no adjacent lysines, whereas the random copolymer has an ensemble of various sequences (see below). These sequence differences are apparent in the ability of the polypeptides to adopt secondary structures in the presence of various solvents. The random $(LAG)_n$ can adopt the α-helical structure in 95% MeOH, hexafluoroisopropyl alcohol, or at high pH, whereas the sequential $(L\text{-}A\text{-}G)_n$ tends to remain in the random conformation (Cernosek et al., 1974a) under all these conditions. The random $(LAG)_n$ copolymer has a statistical distribution which is the result of the dissimilar kinetics of polymerization of the three *N*-carboxyanhydrides. The different polymerization rates would tend to form clusters rather than a random distribution of the amino acids, resulting in an excess of Gly in the C-terminal region of the copolymer, and a high lysine and alanine content in the N-terminal region (Cernosek et al., 1974a; Shalitin and Katchalski, 1960). This asymmetric distribution of amino acids could account for the greater tendency to form secondary structure. The sequential $(L\text{-}A\text{-}G)_n$ has a unique sequence in that all lysines are separated by alanine and glycine. The fact that glycine occurs at every third position tends to favor a more random conformation (Chou and Fasman, 1974). It is not surprising that the random $(LAG)_n$ polymer which has a sequence distribution similar to that of histone H1, in the clustering of lysines and apolar residues, should produce DNA complexes which aggregate and show altered CD spectra similar to Ψ-form DNA as do H1-DNA complexes (Adler and Fasman, 1971; Fasman et al., 1970). Other authors have also reported that differences in the conformation of the free polypeptides in solution may bring about a difference in complex structure with DNA (Sponar et al., 1973; Ong et al., 1976).

Sponar and co-workers (1973, 1975) have also investigated DNA complexes with a sequential polypeptide, $(L\text{-}Ala\text{-}L\text{-}Lys\text{-}L\text{-}Pro)_n$, and have obtained results different from those reported herein. This polypeptide is also in the random conformation in solution. These authors observed similar Ψ-like CD spectra for their polypeptide-DNA complex; however, their complexes precipitate at a lower Lys/nucleotide ratio than reported herein for the $(L\text{-}A\text{-}P)_n$-DNA complex. In addition, the transition in the plot of $[\theta]_{275}$ vs. NaCl occurs at a higher salt concentration than noted for the complex presented here. It is consistent that a polypeptide-DNA complex which precipitates at a lower Lys/nucleotide ratio should show a salt transition at a higher ionic strength. The fact that a lower

amount of polypeptide to DNA can cause condensation and aggregation of the complex suggests that the structural change can occur at higher salt concentration (Mandel and Fasman, 1976; Ong and Fasman, 1976). The difference in these results may be due to the fact that a lysine residue followed by a proline has fewer degrees of freedom than a lysine residue which follows a proline residue (Schimmel and Flory, 1968). It is possible that the greater conformational restriction of the (L-Ala-L-Lys-L-Pro)$_n$ polypeptide relative to the (L-A-P)$_n$ polypeptide may tend to produce different polypeptide conformations for the two sequential polymers when bound to DNA. This difference may induce the condensed forms of DNA at lower Lys/nucleotide ratios or at higher salt for any given Lys/nucleotide ratio for the (L-Ala-L-Lys-L-Pro)-DNA complex relative to the (L-A-P)$_n$-DNA complex due to the enhanced interactions between the DNA bound polypeptide in the former rather than the latter complex.

It is interesting to compare the lack of any scattering or CD spectral changes with the sequential (L-A-G)$_n$-DNA complexes studied herein to a rather dissimilar result with DNA complexes with (L-Lys-Gly-Gly)$_n$ (Williams and Kielland, 1975). This sequential copolymer-DNA complex produced Ψ-like DNA CD spectra, qualitatively similar to the CD of poly(L-lysine)-DNA complexes. Although the two copolymers are both in the random coil conformation in solution, when bound to DNA and neutralized, they caused different DNA CD spectra, probably indicating a different structure of the bound copolymer. A similar change in DNA complex structure, brought about by two copolymers differing only in one amino acid, has been reported (Ong et al., 1976; Mandel and Fasman, 1976; Sponar et al., 1973). For example, L-Lys, L-Leu copolymer complexes with DNA produced strikingly different CD spectra from those with L-Lys, L-Val copolymers. This result is possibly due to the respective helix or β-sheet promoting tendency of these amino acids (Chou and Fasman, 1974).

The complexes of DNA and polypeptides often yield turbid solutions which cause light scattering. The effects of such scattering on the CD spectra have been previously discussed in detail (Shih and Fasman, 1972). By use of the Fluorscat cell (Adler et al., 1975b), it was shown that the CD contribution of such scattering is indeed small and therefore has not been corrected for in the spectra herein.

Salt Dependence CD Spectra of the Complexes. The positive band in the CD spectra of DNA is dependent on the ionic strength of the medium: $[\theta]_{275}$ monotonically increases with decreasing salt (Zama, 1974; Ong et al., 1976). A similar salt dependence of the CD spectra of complexes of (L-A-G)$_n$-DNA at $r = 1$ is seen in Figure 3. This result is consistent with the near identical CD spectra at various r values. It may be inferred that there is little or no DNA structural change in the (L-A-G)$_n$-DNA complex. The ionic strength dependence of the CD spectra of the random (LAG)$_n$-DNA complex (Figure 3) is quite different, and resembles those curves observed with complexes of poly-L-Lys and DNA (Shapiro et al., 1969; Zama, 1974; Mandel and Fasman, 1976), complexes with several L-Lys, L-Leu copolymers and DNA (Ong et al., 1976), L-Lys, L-Ala, L-Pro polypeptides and DNA (Sponar et al., 1973), and complexes of histone H1 and DNA (Fasman et al., 1970; Sponar and Fric, 1972).

The CD spectra vs. NaCl concentration of previously studied polypeptide-DNA complexes all manifest one minimum or one transition; however, the plot of $[\theta]_{275}$ vs. [NaCl] presented here shows two minima, occurring at 0.75 and 0.22 M NaCl (Figure 3). It is suggested that the two minima are a result of the annealing of DNA with a polypeptide having a distribution of adjacent lysines containing both long and short runs, due to the kinetics of polymerization. Histone H1, for which random (LAG)$_n$ is considered an appropriate model, has short sequences of adjacent lysines (or charged residues) (Jones et al., 1974; Rall and Cole, 1971; G. Dixon, private communication). The synthetic polypeptides, studied herein, on the other hand, are polymerized with a larger percentage of lysine and therefore should possess sequences with longer runs of lysine. The histone H1-DNA complex has a salt-dependent CD transition at 0.12 M NaCl (Fasman et al., 1970), while the synthetic polypeptide-DNA complexes have their extrema in the range of 0.8 to 1.0 M NaCl. Consequently, the complex of random (LAG)$_n$-DNA, in which the polypeptide has a probability of having short and long sequences of adjacent lysines, has two minima at low (0.22 M) and high (0.75 M) NaCl.

It has been observed, in this laboratory, that different salts can increase the distortion of the CD spectra of histone H1-DNA complexes (Adler and Fasman, 1971). The guanidinium ion was shown to be the most effective in increasing the conformational change in histone H1-DNA complexes, as monitored by CD, presumably by increasing the formation of asymmetric superstructures. The salt dependence of the CD spectra of (LAG)$_n$-DNA complexes presented here is in conformity with these findings. When GdmHCl, rather than NaCl, is employed in the gradient dialysis, the CD minima observed are more negative (Figure 4). The fact that the minima occur at lower concentrations of GdmHCl than NaCl is probably a consequence of a tighter binding to and therefore shielding of the DNA by the guanidinium cation relative to the Na^+ cation.

The experimental procedure, i.e., method of altering the ionic strength, can produce different ellipticities for complexes of (LAG)$_n$-DNA. By a linear GdmHCl gradient, the interpolated values for $[\theta]_{275}$ at 0.04 and 0.12 M GdmHCl are -2800 and $-14\,500$ deg cm^2 dmol^{-1}, respectively (Figure 4). However, if the same salt concentrations are reached by a step dialysis, positive ellipticities of 4000 and 200 deg cm^2 dmol^{-1}, respectively, are obtained, which are not very different from the ellipticities observed at high ionic strength before the step dialysis. In the gradient method, the DNA and polypeptide adjust to the slow varying ionic strength conditions and interact with unique conformations as a function of the environmental conditions. The procedure of step dialysis or direct mixing causes the DNA and polypeptide to mix and interact under an abrupt change in solution conditions. Because the interaction between two heavily charged macromolecules allows for many modes of binding, and due to the rapid and irreversible kinetics of binding, the DNA and polypeptide will interact in a variety of conformations and binding sites. This type of binding will be of a more statistical type which will be more dependent on the original, premixed, solution conditions, than on the conditions after mixing, and may emphasize the electrostatic interaction over other more subtle modes of binding. It is not surprising that direct mixing often gives nonreproducible results (Adler and Fasman, 1971) and immediate precipitation when performed at low ionic strength (Olins et al., 1968). Rapid mixing also gives different thermal denaturation profiles than those obtained with dialysis (Mandel and Fasman, 1976).

The formation of a Ψ-like condensed DNA, at a given Lys/nucleotide ratio for the (L-A-P)$_n$-DNA complex is also dependent on the ionic strength (Figures 5A and B). With both NaCl and GdmHCl, the formation of condensed DNA spectra in the complex occurs, but the magnitude of the ellipticities

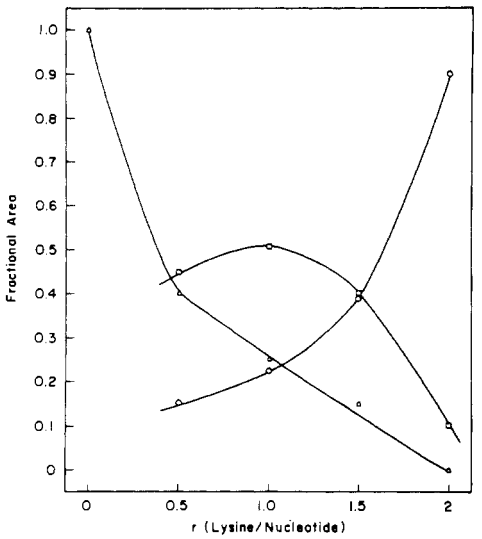

FIGURE 12: Fractional area of derivative hyperchromicity vs. r for (L-Lys-L-Ala-Gly)$_n$-DNA complexes. The thermal derivative hyperchromicity curves of Figure 7 were normalized using a Du Pont 310 curve resolver. T_{mI} (△); T_{mII} (□); T_{mIII} (○). r = Lys/nucleotide ratio.

observed in the presence of GdmHCl is many-fold greater.

The CD spectra of DNA are very sensitive to the conformation of DNA alone (Johnson and Tinoco, 1969; Studdert and Davis, 1974; Cheng and Mohr, 1975) and to the state of condensation of the polypeptide–DNA complex, which in turn is a function of the Lys/nucleotide ratio and salt concentration. The CD spectra of the complex can manifest a Ψ-like pattern at a given r by varying the ionic strength or at a given ionic strength by varying r. This functional dependence implies a unique phase transition to the condensed form analogous to liquid crystal formation discussed previously (Ong et al., 1976). Those polypeptide–DNA complexes, which show no CD changes at a given ionic strength by varying r, likewise show no CD changes beyond those of free DNA, at a given r by varying the ionic strength. Examples of such complexes are DNA with block (L-Lys^{77}) (L-Leu^{23}) (Ong et al., 1976) and sequential poly(L-Lys-L-Ala-Gly), reported herein.

Thermal Denaturation. The thermal denaturation of the polypeptide–DNA complexes was performed using the simultaneous observation of UV hyperchromicity and CD changes described by Mandel and Fasman (1974). The complexes were annealed and studied in 2.5×10^{-4} M EDTA, pH 7.0. The respective UV and CD thermal derivative profiles of sequential (L-A-G)$_n$–DNA complexes are shown in Figures 6 and 7. The presence of three melting zones are noted, corresponding to a polypeptide free DNA region (T_{mI} = 47 °C) and two higher melting zones (T_{mII} = 66 °C, and T_{mIII} = 77 °C), representing polypeptide bound DNA regions (Table I). The fractional areas of the three respective melting regions as a function of r, the input ratio of lysine/nucleotide, are shown in Figure 12. At low r both the central (T_{mII}) and high (T_{mII}) melting zones are present, indicating a stabilization of DNA regions by bound polypeptide. As r increases, both melting zones increase at the expense of the free DNA zone; however, the central melting zone passes through a maximum and then falls as the highest melting zone is further populated. The fact that there are two melting zones representing polypeptide bound DNA implies that the polypeptide has two modes of binding and stabilization of DNA to thermal denaturation. It is at first surprising that the sequential (L-A-G)$_n$ which has a unique trimer distribution should be bound to DNA in two ways. The unique sequence does not contain lysine rich and nonpolar rich regions which might generate two binding modes and therefore two melting zones. A plausible explanation for these observed results is that the polypeptide binds in a moderately cooperative nature to regions of already polypeptide bound DNA. If the polypeptide initially bound randomly only to free DNA, then at intermediate r values one would observe only two melting zones corresponding to free DNA (T_{mI}) and the bound central zone (T_{mII}). If, on the other hand, the polypeptide bound cooperatively to polypeptide bound DNA regions, then at intermediate r values one would observe only free DNA (T_{mI}) and regions of DNA bound by more than one polypeptide (T_{mIII}). The plots in Figure 12 are consistent with a moderately cooperative binding model in which at r = 1 the central melting zone is a maximum and rapidly falls in fractional area as the highest melting zone rises with an increasing positively sloped curve.

There has been considerable evidence in the literature concerning the specificity of lysine-containing model histone polypeptides for DNA specific sequences (Wehling et al., 1975; Leng and Felsenfeld, 1966; von Hippel and McGhee, 1972). Using data from thermal denaturation studies, several authors have shown a lysine specificity for A-T rich regions (Olins et al., 1968; Shapiro et al., 1969; Mandel and Fasman, 1976; Ong and Fasman, 1976), and an arginine specificity for G-C rich regions (Pinkston and Li, 1974; Epstein et al., 1974). Moreover, with regard to calf thymus DNA, Li et al. (1974a) have shown that the high melting shoulder of this DNA corresponds to a 13% fraction of calf thymus DNA (55% G-C). The melting data presented herein show that the free DNA melting zone shifts to higher temperature with increasing r. Similar results have been reported by Santella and Li (1975). In addition, the width of this melting zone sharpens from 10 ± 1 °C to 7 ± 1 °C, in agreement with a G-C rather than A-T rich melting region (Bloomfield, 1968). The breadth of the DNA melting curve is due to the difference in base pair stability; a A-T rich segment is considerably broader than a G-C rich section. It is therefore suggested that sequential (L-A-G)$_n$ binds with greater affinity to A-T rich regions. CD melting profiles usually provide additional information in the premelting region (Gennis and Cantor, 1972) compared with hyperchromism melting profiles; yet, in the case of (L-A-G)$_n$–DNA complexes, the premelt slopes are the same, and there appears to be no ordered dependence of the premelt on r.

The UV and CD thermal denaturation profiles of random (LAG)$_n$–DNA complexes are rather different from those of the sequential (L-A-G)$_n$–DNA complexes. At the ratios of lysine/nucleotide examined there are four melting regions in the denaturation profile of (LAG)$_n$–DNA complexes as compared with three regions for melting profiles of (L-A-G)$_n$–DNA complexes. As seen with the sequential (L-A-G)$_n$–DNA complexes, the statistical (LAG)$_n$–DNA complexes also show a specificity for A-T rich regions. The two central melting regions (T_{mII} and T'_{mII}) in the derivative absorption profile (Figure 8) may correspond to differential stabilization of the DNA by regions of the random polypeptides differing in the ratio of lysine to nonpolar residues. The highest melting region (T_{mIII}), occurring at approximately 92 °C, has been observed with other lysine copolymer–DNA complexes having a high degree of contiguous lysine residues (Olins et al., 1968; Pinkston and Li, 1974; Santella and Li, 1974; Mandel and Fasman, 1976; Ong and Fasman, 1976). The complex CD melting profile, shown in Figure 9, attests to the necessity of additional information in interpreting thermal denaturation based exclusively on UV hyperchromism. In the CD thermal

profiles of sequential $(L\text{-}A\text{-}G)_n$–DNA complexes, there is a premelt region followed by a decrease in ellipticity, corresponding to melting of free and polypeptide-bound DNA regions. However, in the melting of random $(LAG)_n$–DNA complexes, the $[\theta]_{280}$ rises sharply between 75 and 90 °C. A similar sharp rise in ellipticity at the highest temperature melting zone has been observed with poly(L-lysine)–DNA complexes (Mandel and Fasman, 1976), L-lysine, L-leucine copolymer–DNA complexes (Ong and Fasman, 1976), and with nucleoprotein containing certain bound histones (Wilhelm et al., 1974a,b).

It is proposed that this CD change is caused by the denaturation of the long-range order or the condensed DNA in the random $(LAG)_n$–DNA complex. This long-range asymmetry must have the opposite chirality to that of double-stranded DNA, for when it is melted out there is an *increase* in the measured ellipticity. Thus the higher ordered structure of the DNA is maintained even at higher temperatures than those necessary to melt free DNA and weakly polypeptide bound DNA regions. The reverse process was reported for the melting of Ψ DNA stabilized by polyethylene oxide and NaCl (Cheng and Mohr, 1974, 1976). These authors observe the melting of the higher order Ψ structure before the melting of the duplex. It is not unreasonable to expect, however, that the higher ordered DNA structure, stabilized by bound polypeptide, is more thermally resistant to denaturation than the Ψ DNA structure brought about by excluded volume effects. Moreover, the low-temperature melting regions have identical T_m's, measured in both the CD and UV mode; the higher temperature melting regions show noncoincidental T_m's, implying that the two techniques are monitoring different but related physical events as the ordered structure is melted. With increasing r, in the $(LAG)_n$–DNA complexes, the fractional area on the derivative UV melting profiles shows a decrease in T'_{II} and an increase in T_{II} melting regions. If T_{mII} and T'_{mII} are a consequence of the binding to DNA by regions of the random polypeptides having lower and higher ratios of lysine to nonpolar residues, then it appears that it is the regions of high lysine to nonpolar residues which are necessary for DNA condensation.

Thermal Denaturation of the Complex. The thermal denaturation profiles of the sequential polypeptide $(L\text{-}A\text{-}P)_n$–DNA complex at 2.5×10^{-4} M EDTA, pH 7.0, at varying Lys/nucleotide ratios are shown in Figures 11A and B. From the thermal derivative UV profile, at intermediate r values, the melting is seen to occur over three transitions: 45–55 °C (T_{mI}), 64–70 °C (T_{mII}), and 76–80 °C (T_{mIII}) (Table II). The first melting transition corresponds to polypeptide-free DNA regions within the complex in agreement with previous studies (Mandel and Fasman, 1976; Ong and Fasman, 1976). This melting region decreases with increasing r indicating further stabilization of DNA by bound polypeptide and is shifted to higher melting regions. The two higher melting regions, representing denaturation of polypeptide bound DNA, show an increase in their respective areas with increasing Lys/nucleotide ratio. However, the central melting region (T_{mII}) passes through a maximum in fractional area similar to the situation observed with $(L\text{-}A\text{-}G)_n$–DNA. Furthermore this sequential polypeptide which has a unique trimer distribution appears to possess two modes of binding and stabilization of DNA. In an analogous manner to this complex, $(L\text{-}A\text{-}P)_n$–DNA also shifts the free DNA melting region toward higher temperatures and narrower melting widths with increasing r. Thus, these two sequential polypeptides are comparable in their ability to bind in a moderately cooperative nature to DNA and to preferentially select A-T rich regions. Nevertheless, the presence of Pro rather than Gly appears to produce unique differences. The fact that $(L\text{-}A\text{-}G)_n$–DNA complexes do not precipitate nor undergo condensation whereas $(L\text{-}A\text{-}P)_n$–DNA complexes do has already been discussed. The thermal denaturation data indicate that complete saturation of the DNA by polypeptide, i.e., the point at which only the high melting transition is observed in thermal denaturation, occurs at approximately $r = 2$ for $(L\text{-}A\text{-}G)_n$–DNA, and at $r = 1.0$ (not shown) for $(L\text{-}A\text{-}P)_n$–DNA. In addition, in terms of the relative amount of free DNA available in the complex, there is no free DNA melting region at $r = 0.8$ for $(L\text{-}A\text{-}P)_n$–DNA; yet at $r = 1$ for $(L\text{-}A\text{-}G)_n$–DNA, the free DNA melting region accounts for over 20% of the entire denaturation. This result is consistent with the suggestion that the condensation of DNA is brought about by the bound polypeptide interactions in the $(L\text{-}A\text{-}P)_n$–DNA complex whereas these interactions do not occur in the $(L\text{-}A\text{-}G)_n$–DNA complex. Thus, for $(L\text{-}A\text{-}P)_n$–DNA at $r = 0.8$, the DNA is condensed and there is no contribution of free DNA; for $(L\text{-}A\text{-}G)_n$–DNA at $r = 1$, due to the moderately cooperative binding there remains a portion of free DNA in the noncondensed complex.

The binding of $(L\text{-}A\text{-}P)_n$–DNA affects other physical parameters of the thermal denaturation. The overall hyperchromicity of DNA is approximately 38% (Li et al., 1974a,b), whereas the hyperchromicity of the $(L\text{-}A\text{-}P)_n$–DNA complexes is approximately 48%. The CD ellipticity difference between the maximum ellipticity and its value after denaturation is ~2000 deg cm^2 dmol^{-1} for DNA, and ~3600 deg cm^2 dmol^{-1} for the $(L\text{-}A\text{-}P)_n$–DNA complexes at $r \geq 0.4$. The residual hypochromicity, namely, the hypochromicity of the sample after it is melted and recooled to its initial temperature, is also affected by the presence of polypeptide. For DNA alone the hyperchromicity is 26% of the theoretical reversible reaction, whereas it is ~35% for the $r = 0.4$ complex, and ~45% for the $r = 1.2$ complex. These results suggest that the polypeptide enhances the formation of duplex upon cooling.

The CD changes with temperature show, beyond the initial premelt, a monotonically decreasing profile for all complexes studied. The CD spectra of the complexes at room temperature, at 2.5×10^{-4} M EDTA, pH 7.0, were all of the usual B-form DNA CD spectra with $[\theta]_{280} \simeq 8500$ deg cm^2 dmol^{-1}, and the solutions were optically clear. This pattern in the denaturation profile indicates that, under these solution conditions, there is no condensed superstructure in the complex. Other examples of complexes manifesting a B-form DNA CD spectrum and a simple melting profile are those with DNA and block (L-Lys^{77}) (L-Leu^{23}) polypeptide (Ong and Fasman, 1976) and sequential $(L\text{-}A\text{-}G)_n$. Other DNA complexes with poly(L-Lys) or (L-Lys, L-Val) polypeptides (Mandel and Fasman, 1976), with (L-Lys, L-Leu) polypeptides (Ong and Fasman, 1976), with random poly(L-Lys, L-Ala, Gly) and chromatin show nonconservative CD spectra at room temperature and a complex denaturation profile indicating the melting out of a condensed form. From the fact that a condensed state of $(L\text{-}A\text{-}P)_n$–DNA is observed by CD at a higher ionic strength, but none by thermal denaturation at low ionic strength is further proof as to the dependence of the compact structure on polypeptide–DNA ratio and salt concentration.

From an analysis of the polypeptides utilized in the complexes, which contain various amino acids and sequences, it is necessary to consider contributions other than electrostatic in describing the protein–DNA and protein–protein interactions leading to the condensation of DNA. Thus, while homo, block, statistical, and sequential lysine containing polypeptides may

induce the condensed Ψ-form DNA, the solution parameters such as the ratio of polypeptide to DNA and the salt concentration at which the transition occurs are different. These differences are due to forces (hydrophobic), besides those of lysine–phosphate charge interaction, which modulate the nature of polypeptide–DNA complex structure and condensation.

Recently great efforts have been made toward the elucidation of chromatin structure. These investigations support a model in which the various histones interact specifically and complex with DNA causing a condensed, ordered, and discrete unit of deoxynucleoprotein (Kornberg and Thomas, 1974). The particulate nature of chromatin was further elucidated by electron microscopy, which showed linear arrays of repeating units [called "ν bodies" by Olins and Olins (1974) or nucleosomes by Oudet et al. (1975)]. Recent neutron scattering studies have led to a globular model in which the histones form a central core and DNA is wound on the core surface (Baldwin et al., 1975; Pardon et al., 1975).

From the thermal denaturation of nucleoprotein studied by Wilhelm and co-workers (Wilhelm et al., 1974a,b), it is clear that, as histones are removed from nucleoprotein, the CD melting profile changes dramatically from that pattern observed with the random $(LAG)_n$–DNA complexes to that observed with the sequential $(L\text{-}A\text{-}G)_n$–DNA complexes. Thus, it is possible to interpret the melting profiles of nucleoprotein as initially the denaturation of unbound DNA regions which precedes the melting of weakly stabilized DNA within the ordered superstructure. The partial unfolding of DNA within the superstructure initiates the collapse of this tertiary structure which is then followed by the complete denaturation of the DNA. If some of the histones are removed, as, for example, by deoxycholate or NaCl (Wilhelm et al., 1974a,b) or the histone–histone interaction is disturbed by solvent conditions such as urea (Bartley and Chalkley, 1973; Chang and Li, 1974; Carlson et al., 1975), the ordered condensed DNA structure is grossly perturbed or lost. By analogy with complexes of DNA and model histone polypeptides, therefore, it has been demonstrated that the CD spectra and thermal denaturation of nucleoprotein support a model in which histone–histone interaction is crucial in the condensation of DNA into higher ordered tertiary structures.

Acknowledgment

The authors thank Drs. A. Adler and R. Mandel for many helpful discussions.

References

Adler, A. J., and Fasman, G. D. (1971), *J. Phys. Chem. 75,* 1516.
Adler, A. J., Fulmer, A. W., and Fasman, G. D. (1975a), *Biochemistry 14,* 1445.
Adler, A. J., Moran, E. C., and Fasman, G. D. (1975b), *Biochemistry 14,* 4179.
Adler, A. J., Ross, D. G., Chen, K., Stafford, P. A., Woiszwillo, M. J., and Fasman, G. D. (1974), *Biochemistry 13,* 616.
Adler, A. J., Schaffhausen, B., Langan, T. A., and Fasman, G. D. (1971), *Biochemistry 10,* 909.
Ansevin, A. T., and Brown, B. W. (1971), *Biochemistry 10,* 1133.
Ansevin, A. T., Hnilica, L. S., Spelsberg, T. C., and Kehm, S. L. (1971), *Biochemistry 10,* 4793.
Baldwin, J. P., Boseley, P. G., Bradbury, E. M., and Ibel, K. (1975), *Nature (London) 253,* 245.
Bartley, J., and Chalkley, R. (1973), *Biochemistry 12,* 468.
Bloomfield, V. (1968), *Biopolymers 6,* 1368.
Carlson, R. D., Olins, A. L., and Olins, D. E. (1975), *Biochemistry 14,* 3122.
Carroll, D. (1971), *Anal. Biochem. 44,* 496.
Cernosek, S. F., Jr., Malin, M., Wells, M., and Fasman, G. D. (1974a), *Biochemistry 13,* 1252.
Cernosek, S. F., Jr., Wells, M., and Fasman, G. D. (1974b), *Isr. J. Chem. 12,* 47.
Chang, C., and Li, H. J. (1974), *Nucleic Acids Res. 1,* 945.
Cheng, S. M., and Mohr, S. C. (1974), *FEBS Lett. 49,* 37.
Cheng, S. M., and Mohr, S. C. (1975), *Biopolymers 14,* 663.
Chou, P., and Fasman, G. D. (1974), *Biochemistry 13,* 222.
Elgin, S. C. R., and Weintraub, H. (1975), *Annu. Rev. Biochem. 44,* 725.
Epstein, P., Yu, S. S., and Li, H. J. (1974), *Biochemistry 13,* 3706.
Fasman, G. D., Schaffhausen, B., Goldsmith, L., and Adler, A. J. (1970), *Biochemistry 9,* 2814.
Gennis, R. B., and Cantor, C. R. (1972), *J. Mol. Biol. 65,* 381.
Johnson, W. C., Jr., and Tinoco, I., Jr. (1969), *Biopolymers 7,* 727.
Jones, G. M. T., Rall, S. C., and Cole, R. D. (1974), *J. Biol. Chem. 249,* 2548.
Jordan, C. F., Lerman, L. S., and Venable, J. H. (1972), *Nature (London), New Biol. 236,* 67.
Kornberg, R. D., and Thomas, J. O. (1974), *Science 184,* 865.
Lang, C. A. (1958), *Anal. Chem. 20,* 1692.
Leng, M., and Felsenfeld, G. (1966), *Proc. Natl. Acad. Sci. U.S.A. 56,* 1325.
Li, H. J., Brand, B., and Rotter, A. (1974a), *Nucleic Acids Res. 1,* 257.
Li, H. J., Brand, B., Rotter, A., Chang, C., and Weiskopf, M. (1974b), *Biopolymers 13,* 1681.
Mandel, R., and Fasman, G. D. (1974), *Biochem. Biophys. Res. Commun. 59,* 672.
Mandel, R., and Fasman, G. D. (1976), *Biochemistry 15,* 3122.
Maniatis, T., Venable, J. H., Jr., and Lerman, L. S. (1974), *J. Mol. Biol. 84,* 37.
Olins, A., and Olins, D. E. (1974), *Science 183,* 330.
Olins, D. E., Olins, A., and von Hippel, P. (1968), *J. Mol. Biol. 33,* 265.
Ong, E., and Fasman, G. D. (1976), *Biochemistry 15,* 477.
Ong, E., Snell, C., and Fasman, G. D. (1976), *Biochemistry 15,* 468.
Oudet, P., Gross-Bellard, M., and Chambon, P. (1975), *Cell 4,* 281.
Pardon, J. F., Worcester, D. L., Wooley, J. C., Tatchell, K., Van Holde, K. E., and Richards, B. M. (1975), *Nucleic Acids Res. 2,* 2163.
Pinkston, M. F., and Li, H. J. (1974), *Biochemistry 13,* 5227.
Privat, J. P., Spach, G., and Leng, M. (1972), *Eur. J. Biochem. 26,* 90.
Rall, S. C., and Cole, R. D. (1971), *J. Biol. Chem. 246,* 7175.
Santella, R. M., and Li, H. J. (1974), *Biopolymers 13,* 1909.
Santella, R. M., and Li, H. J. (1975), *Biochemistry 14,* 3604.
Schimmel, R. R., and Flory, P. (1968), *J. Mol. Biol. 34,* 105.

Shalitin, Y., and Katchalski, E. (1960), *J. Am. Chem. Soc. 82,* 1630.
Shapiro, J. T., Leng, M., and Felsenfeld, G. (1969), *Biochemistry 8,* 3219.
Shih, T., and Fasman, G. D. (1971), *Biochemistry 10,* 1675.
Shih, T. Y., and Fasman, G. D. (1972), *Biochemistry 11,* 398.
Sponar, J., Blaha, K., and Stokrova, S. (973), *Stud. Biophys. 50,* 125.
Sponar, J., and Fric, I. (1972), *Biopolymers 11,* 2317.
Sponar, J., Fric, I., and Blaha, K. B. (1975), *Biophys. Chem. 3,* 255.
Stokrova, S., Sponar, J., Havranek, M., Sedlacek, B., and Blaha, K. (1975), *Biopolymers 14,* 1237.
Studdert, D. S., and Davis, R. C. (1974), *Biopolymers 13,* 1377.
von Hippel, D. H., and McGhee, J. D. (1972), *Annu. Rev. Biochem. 41,* 231.
Wehling, K., Arfman, H., Standke, K. C., and Wagner, K. G. (1975), *Nucleic Acids Res. 2,* 799.
Wilhelm, F. X., De Murcia, G. M., Champagne, M. H., and Daune, M. P. (1974a), *Eur. J. Biochem. 45,* 431.
Wilhelm, F. X., De Murcia, G. M., and Daune, M. P. (1974b), *Nucleic Acids Res. 1,* 1043.
Williams, R. F., and Kielland, S. L. (1975), *Can. J. Chem. 53,* 542.
Zama, M. (1974), *Biochim. Biophys. Acta 366,* 124.

Ethoxyformylation and Photooxidation of Histidines in Transferrins†

Terry B. Rogers, Robert A. Gold,‡ and Robert E. Feeney*

ABSTRACT: The chemical reactivity of histidines in ovotransferrin and human serum transferrin was studied utilizing two different reactions. Upon dye-sensitized photooxidation of ovotransferrin and ethoxyformylation of human serum transferrin and ovotransferrin, losses in histidine and iron-binding activity were observed. All of the histidines in both apoproteins could be ethoxyformylated by the use of 170 to 400 molar excesses of reagent resulting in complete loss in activity. The histidines of human serum transferrin showed a greater reactivity toward the reagent than did those of ovotransferrin. The binding of each iron protected two histidines from ethoxyformylation, and in both cases the proteins remained completely active. First-order losses in histidine and iron-binding activity were observed when ovotransferrin was irradiated in the presence of methylene blue. Comparison of the first-order rates indicates the loss of two histidines per binding site accounts for the inactivation of the protein. However, iron binding did not protect ovotransferrin from photoinactivation as expected. Evidence from both modification techniques indicates: (1) Histidines are essential for iron-binding activity. (2) There are two essential histidines in each binding site. The advantages of using two modification reactions, ethoxyformylation and photooxidation, in the study of the functional role of histidines in proteins are demonstrated in this work.

The transferrins are a class of vertebrate glycoproteins which chelate iron in two specific sites on each molecule. Chemical modification is a technique that has been very useful in studying the iron-binding sites of the transferrins. *N*-Acetylimidazole (Komatsu and Feeney, 1967), tetranitromethane (Tsao et al., 1974; Line et al., 1967), and iodine (Komatsu and Feeney, 1967; Azari and Feeney, 1961; Phillips and Azari, 1972) modifications have implicated tyrosine residues as essential for iron binding. Spectroscopic studies have shown that there is at least one nitrogen coordinated to the metal in the binding center and perhaps as many as three are involved (Spartalian et al., 1973; Windle et al., 1963). EPR[1] studies on copper-transferrin complexes indicate that there are as many as four nitrogens available for coordination in the iron-binding site (Aasa and Aisen, 1968).

A number of nitrogen-containing amino acid side chains have been excluded as essential for the activity of the transferrins. Reductive alkylation and trinitrophenylation of human serum transferrin (Means and Feeney, 1968; Zschocke et al., 1972) as well as succinylation and acetylation of chicken ovotransferrin (Buttkus et al., 1965) indicate that amino groups are not directly essential for activity but may be important to the conformational integrity of the protein. Tryptophan is considered nonessential from the chemical-modification studies of human serum transferrin with 2-hydroxy-5-nitrobenzyl bromide (Ford-Hutchinson and Perkins, 1972).

Chemical studies on human serum transferrin with bromoacetate, 5-diazonium-1*H*-tetrazole (Line et al., 1967) and, more recently, ethoxyformic anhydride (Krysteva et al., 1975) have implicated histidines in the metal-binding center. The conclusion that there are two histidines per binding site, derived from the bromoacetate reaction data, is questionable, since the iron-binding activity is rapidly lost only after more than ten residues have been carboxymethylated; yet, the apparent random reaction of histidines shows no such cooperative effect.

† From the Department of Food Science and Technology, University of California, Davis, California 95616. *Received December 7, 1976.* This work was supported in part by Grants HD 00122 and HL 18619 from the National Institutes of Health. This material constitutes part of the thesis of T.B.R. submitted to the Graduate Division of the University of California at Davis in partial fulfillment of the requirements for a Ph.D. degree in Agricultural Chemistry and part of the thesis of R.A.G. for a M.S. degree in Biochemistry.

‡ Present address: School of Medicine, University of Monterrey, Monterrey, Mexico.

[1] Abbreviations used are: Fe-NTA, iron nitrilotriacetate; EDTA, (ethylenedinitrilo)tetraacetic acid; EPR, electron paramagnetic resonance.